PROGRESSIVE AND LOSSLESS IMAGE CODING USING OPTIMIZED NONLINEAR SUBBAND DECOMPOSITIONS

A. Benazza-Benyahia

Ecole Supérieure des Communications,
LS Télécoms,
3.5 Km Route de Raoued,
2083 Cité El-Ghazala,
Tunisia.
Email: ben.yahia@planet.tn

J-.C. Pesquet

LSS-CNRS/ Univ. Paris 11,
ESE, Plateau de Moulon,
91192 Gif-sur-Yvette Cédex,
France.
Email: pesquet@lss.supelec.fr

ABSTRACT

In super high-definition image applications such as medical image archival, progressive and lossless coding is required since any degradation in the decompressed image is unacceptable. Recently, nonlinear subband decompositions have received much attention as they provide very compact multiresolution representations and they allow exact reconstruction of the input image. Within this framework, we propose to design optimized decompositions adapted to the variations of the statistics of the images under study. Comparative investigations are performed by simulations, indicating that the proposed decompositions outperform the existing lossless compression techniques.

1. INTRODUCTION

Progressive image transmission is recommended for image data retrieval and telebrowsing of image databases [1]: an approximation of the image is rapidly displayed and refined gradually until the original image is obtained. Multiresolution decompositions [2] and pyramidal algorithms [3] have been extensively used for compression owing to their progressiveness. An appropriate choice of the decomposition reduces the entropy in the subbands and the progressive coding is performed by sequentially transmitting the subbands starting from the lowest resolution subimage. However, coders based on such linear subband decomposition are generally lossy since the coefficients have to be rounded and quantized before the entropy coding stage. In certain fields such as medical image coding or military satellite imaging, using reconstructed images with (even small) artifacts are not acceptable since they may lead to erroneous diagnoses. In such areas, a lossless coding is required. Therefore, in the context of exact coding, the decomposition must achieve perfect reconstruction from the quantized coefficients, which is not in general an easy task.

Recently, a solution to the problem was provided thanks to new wavelet transforms that map integers to integers (see e.g. [4, 5, 6, 7]). These ones represent a nonlinear extension of the wavelet decomposition [8] which use the lifting scheme for rounding off the resulting coefficients. The proposed schemes involve fixed operators which are not necessarily best adapted to the image contents. The main motivation of our present work is to optimize these operators in order to track the statistical variations of the input signal. As proposed in [9], we expect to increase the compression ratio by such an optimization step.

This paper is organized as follows. Section 2 introduces the nonlinear subband decomposition for a multiresolution representation of the image. Section 3 addresses both problems of optimization of the parameters of the considered decomposition and entropy coding of the resulting subbands. Finally, the results of our simulations are presented and some conclusions are drawn in Section 4.

2. NONLINEAR SUBBAND DECOMPOSITION

The 1D nonlinear subband decomposition structure is depicted in Fig. 1 [10]. We initialize the decomposition process by setting $c_0(n) = x(n)$, where $x(n)$ denotes the signal to be coded. By an appropriate choice of the operators $\mathcal{H}$ and $\mathcal{G}$, the coefficients $c_j(n)$ may be viewed as the approximation coefficients of the signal at resolution level j whereas $d_j(n)$ are associated to the

This work was partly supported by the CNRS contract France/Tunisia "Réseau No. 12/041/TN".

details lost when passing from resolution level j to the next coarser one $(j+1)$. The two subband signal $c_j(n)$ and $d_j(n)$ are given by:

$$\left\{ \begin{array}{lcl} d_{j+1}(n) & = & \mathcal{A}_2\left[c_j(2n) - \mathcal{H}[\mathbf{c}_j(2n+1)]\right] \\ c_{j+1}(n) & = & \mathcal{A}_1\left[c_j(2n+1) + \mathcal{G}[\mathcal{A}_2^{-1}[\mathbf{d}_{j+1}(n)]]\right] \end{array} \right. , \tag{1}$$

where $\mathbf{c}_j(n) \stackrel{\triangle}{=} (c_j(n+2k))_{-N_1 \leq k \leq N_2}$ and $\mathbf{d}_j(n) \stackrel{\triangle}{=} (d_j(n+k))_{-N'_1 \leq k \leq N'_2}$. Such nonlinear extensions of the wavelet decomposition with critical subsampling allow an exact reconstruction provided that $\mathcal{A}_1$ and $\mathcal{A}_2$ are one-to-one mappings [10]. Indeed, the analysis filter bank in Fig. 1 is associated to a dual synthesis filter bank in a straightforward manner since the following reconstruction equations are satisfied:

$$\left\{ \begin{array}{lcl} c_j(2n+1) & = & \mathcal{A}_1^{-1}[c_{j+1}(n)] - \mathcal{G}[\mathcal{A}_2^{-1}[\mathbf{d}_{j+1}(n)]] \\ c_j(2n) & = & \mathcal{A}_2^{-1}[d_{j+1}(n)] + \mathcal{H}[\mathbf{c}_j(2n+1)] \end{array} \right. . \tag{2}$$

The perfect reconstruction in only due to the intrinsic structure of the decomposition. The approximation signal is recursively processed over j_m resolution levels and a pyramid representation is built in this way. Extension to 2D signal can be obtained by decomposing first the rows then the columns of the image. However, reversing the order of the processing does not lead to the same decomposition because of the nonlinearity of the operators.

The performance of the decomposition is closely related to the choice of operators $\mathcal{H}$ and $\mathcal{G}$. Several two-band decomposition have been investigated in our previous works [6, 11]. One competitive two-band decomposition - which we call NL - consists in introducing nonlinear roundoff in each lifting steps:

$$\left\{ \begin{array}{l} d_{j+1}(n) = c_j(2n) - \lfloor \mathbf{a}_j^T \mathbf{c}_j(2n+1) \rceil \\ c_{j+1}(n) = c_j(2n+1) + \lfloor \frac{1}{4}(d_{j+1}(n-1) + d_{j+1}(n)) \rceil \end{array} \right. \tag{3}$$

where $\lfloor \cdot \rceil$ denotes the rounding operation. It should be noted that the coefficients of the vector $\mathbf{a}_j$ are not necessarily integers so floating point operations can be used to compute the integer coefficients $d_{j+1}(n)$ and $c_{j+1}(n)$. We can interpret $d_{j+1}(n)$ as the error of prediction of the even samples by the odd ones. The update step in evaluating $c_{j+1}(n)$ provides a smoother low-pass signal as compared to direct down-sampling $c_{j+1}(n) = c_j(2n)$.

In this study, we focus on optimal determination of the weighting vector $\mathbf{a}_j$ for a more efficient compression.

3. OPTIMIZATION

The effectiveness of the lossless coding is measured by the zero-th order entropy H which is a weighted sum of the entropies of the approximation and detail subimages. The more the entropy is decreased, the more compact the resulting representation is. Therefore, a first solution consists in minimizing the entropy of the pyramidal representation. The problem is that the entropy is an implicit function of the parameters of the decomposition.

To solve this problem, we have used the Nelder-Mead simplex algorithm [12] but its main drawback is a very heavy computational load. So, other alternatives have been investigated.

In particular, it is possible to calculate the coefficients $\mathbf{a}_j$ that minimize the variance of the detail coefficients $d_{j+1}(n)$. It should be noted that this method does not necessarily minimize the entropy. Its main advantage is its computational feasibility. By using optimum linear prediction theory, the Yule-Walker equations are obtained. However, the normal equations hold under the assumption of stationarity of the analyzed signal, which is not generally valid for images. To track the local variations of the statistics of the input image, the predictor $\mathbf{a}_j$ is made adaptive. The coefficients of the predictor $\mathbf{a}_j$ are updated according to the following normalized LMS adaptation rule:

$$\mathbf{a}_j(n+1) = \mathbf{a}_j(n) + \frac{\mu}{\lambda + ||\mathbf{c}_j(2n+1)||^2} d_{j+1}(n)\mathbf{c}_j(2n+1). \tag{4}$$

To avoid the transmission of the predictor coefficients as side information, an adaptive backward configuration is adopted.

Furthermore, it is known that the coarsest approximation signal at the final resolution level j_m has statistical properties similar to those of the original input image. A classical DPCM with intra-image prediction based on the three causal nearest neighbors can be carried out and integrated within the operator $\mathcal{A}_1$ in Fig. 1. Another monoresolution coding technique could be applied for a more efficient decorrelation of the root approximation subimage as for example, the coder LOCO-I, associated to the current standard of lossless coding JPEG-LS [13]. We denote by NL* the NL decomposition combined with a DPCM coding of the coarsest approximation sub-image.

Once the image has been decomposed, the resulting coefficients must be encoded in order to generate a bitstream. In the literature, subband entropy coding requires sophisticated encoding techniques based on zerotree schemes like the embedded zerotrees decomposition [14] or the set partionning in hierarchical tree [4]. It has been noted that the use of successive refinements to create embedded bit streams becomes somewhat computationally expansive for lossless coding [15]. Thus, following the choices made for the future compression standard JPEG-2000 currently developped by the ISO, we do not employ an embedded coder [16]. More precisely, each subband is coded independently of the others. The main drawback is that we do not exploit the eventual correlations between subbands through the stages of the pyramidal representation. However, there are numerous benefits and the most important ones are the simplicity of the implementation and a better error resilience, especially in the case of progressive transmission over noisy channels. Furthermore, for applications of telebrowsing such as teleradiology, rate scalability is preferred to quality scalability. A coarse version of the images can be recovered by decoding rapidly each detail subimages.

4. EXPERIMENTAL RESULTS

The considered decomposition was carried out on test images of different types, initially coded with 8 bpp. Here, we report the results for the 512×512 image "Lena" and the 256×256 image "Boat". The initial entropies are respectiveley $H_0 = 7.4451$ and $H_0 = 7.5747$. The choice of the number of levels j_m corresponds to a trade-off between the decorrelation ability of the pyramidal representation and the efficiency of the entropy coder. Indeed, the efficiency of entropy coders depends on the length and the statistics of the input sequence. For this reason, entropy coders do not perform well in the case of small sub-images. Furthermore, it is recommended to limit the number of stages of the decomposition in the context of progressive transmission because the receiver is not able to recognize rapidly and reliably images of small size at a coarse resolution. Thus, on each image, we performed a $j_m = 3$ stages decomposition.

The effectiveness of the considered decompositions is measured by both the zero-th order entropy H and the bit-rate r. The compression ratio T_c is derived from compressed file sizes ($r = 8/T_c$). In our experiments, we just employed an adaptive Huffman coder since it is easy to implement and its decoding is very fast. Obviously, an improvement should be expected by using context-coders as proposed in [15], [16]. As a reference, performances of the (monoresolution) lossless modes of the standard JPEG [17] are reported in tables 1 and 2. Tables 3 and 4 contain the performances of several pyramidal decompositions. We denote by $(N, \tilde{N})$ the wavelet transforms that map integers to integers, proposed by Calderbank *et al.* [5]. The numbers $N, \tilde{N}$ correspond repectively to the number of vanishing moments of the analyzing (resp. synthesizing) high pass filters. The transforms S and S+P correspond respectively to the sequential transform and the sequential plus predictive decomposition [4]. For the decomposition NL and NL*, in the case of fixed predictors, we used level-dependent predictors obtained by a Nelder-Mead algorithm. Some conclusions can be drawn from Tables 3 and 4. There is no single transform that perfoms best over the test images if we except NL*. In the case of the "Boat" image, it should be emphasized that the optimized version of the nonlinear decomposition NL can lead to a significant decrease in entropy with respect to both the monoresolution cases and to the other nonlinear subband decomposition currently reported in the literature [4, 5]. However, Tables 3 4 show that it is not always useful to spatially adapt any decomposition within a given image. For instance, adapting the predictor of the (4,2) and the (4,4) transforms decreases the entropy for "Boat" but increases the entropy for "Lena". Finally, in Figure 2, the approximation sub-image at the second level are shown. It can be seen that the S+P transform provides quite a smooth images while the proposed nonlinear decomposition lead to a slightly sharper result. For real compression schemes, adaptive Huffman entropy coders can be used and we have compared the associated bit rates. The results are tabulated in Table 5. They suggest that an improvement could be expected by using a more sophisticated coder than the adaptive Huffman entropy coder.

5. REFERENCES

[1] K.H. Tzou, "Progressive image transmission: a review and comparison of techniques", *Optical Engineering*, 26(7), 581-589, July 1987.

[2] M. Antonini, M. Barlaud, P. Mathieu, I. Daubechies, "Image coding using wavelet transform", *IEEE Trans. on Image Processing*, 1(2), 205-220, April 1992.

[3] P.J. Burt, E.H. Adelson, "The Laplacian pyramid as a compact image code", *IEEE Trans. Commun.*, 31(4), 532-540, April 1983.

[4] A. Said, W.A. Pearlman, "An image multiresolution representation for lossless and lossy compression", *IEEE Trans. on Image Processing*, 5(9), 1303-1310, September 1996.

[5] A.R. Calderbank, I. Daubechies, W. Sweldens, B.-L. Yeo, "Wavelet transforms that map integers to inte-

gers", *Applied and Computational Harmonic Analysis*, 5(3), 332-369, July 1998.

[6] F.J. Hampson, *Nonlinear methods for image coding and motion estimation*, Ph. D. Thesis, University of Paris XI Orsay, France, July 1997.

[7] R.L. de Queiroz, D.A.F. Florêncio, R.W. Schafer, "Non-expansive pyramid for image coding using a nonlinear filter bank", *IEEE Trans. on Image Processing*, 7(2), 246-252, February 1998.

[8] S. Mallat, "A theory for multiresolution signal decomposition: the wavelet representation", *IEEE Trans. on Pattern Analysis and Machine Intelligence*, 11(7), 674-693, July 1989.

[9] O.N. Gerek, A.E. Çetin, "Polyphase adaptive filter banks for fingerprint image compression", *Eureopean Signal Processing Conference*, Rhodes Islands (Greece), 45-48, September 1998.

[10] F.J. Hampson, J.C. Pesquet, "M-band nonlinear subband decompositions with perfect reconstruction", *IEEE Trans. on Image Processing*, 7, 1547-1560, November 1998.

[11] A. Benazza-Benyahia, F.J. Hampson, J-.C. Pesquet, "Progressive and lossless image coding using rank-order filters", *International Conference on Signal Processing and Communications*, Gran Canarias (Spain), 341-344, February 1998.

[12] W. H. Press, B. P. Flannery , S.A. Teukolsky, W. T. Vetterling, *Numerical recipes: the art of scientific programming*, Cambridge, UK: Cambridge Univ. Press. 1986.

[13] M.J. Weinberger, G. Seroussi, G. Sapiro, "LOCO-I: a low complexity, contetx-based, lossless image compression algorithm", *Proc. Data Compression Conference*, Snowbird, (USA), 140-149, March 1996.

[14] J. M. Shapiro, "Embedded image coding using zerotrees of wavelets coefficients", *IEEE Trans. Signal Processing*, 41, 3445-3462, December 1993.

[15] N. Memon, X. Wu, B.-L. Yeo, " Improved techniques for lossless image compression with reversible integer wavelet transforms", *International Conference on Image Processing*, Chicago, (USA), 3, 891-895, October 1998.

[16] F. Sheng, A. Bilgin, P.J. Sementilli, M.W. Marcellin, "Lossy and lossless image compression using reversible integer wavelet transforms", *International Conference on Image Processing*, Chicago, (USA), 3, 876-880, October 1998.

[17] G. Wallace, "Overview of the JPEG (ISO/CCITT) still image compression standard" in *Image processing algorithms and techniques*, SPIE Editor, 1244, 220-233, 1990.

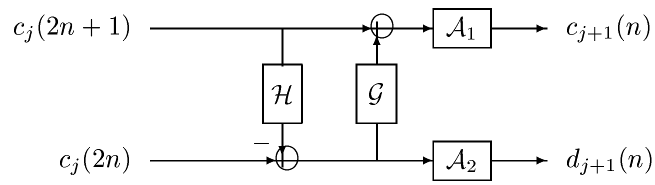

Figure 1: Nonlinear subband decomposition.

Technique	H	r (bpp)	T_c
JPEG #2	4.6596	4.6542	1.7188
JPEG #4	4.7974	4.7885	1.6707
JPEG #5	4.7192	4.7117	1.6959
JPEG #6	**4.575**	**4.5650**	**1.7524**
JPEG #7	4.6063	4.6044	1.7375

Table 1: Performances of monoresolution lossless coding methods corresponding to the 512×512 "Lena" image (initial entropy $H_0 = 7.4451$).

Technique	H	r (bpp)	T_c
JPEG #2	5.3774	5.4335	1.4724
JPEG #4	5.2726	5.3143	1.5054
JPEG #5	5.3198	5.3660	1.4909
JPEG #6	**5.1530**	**5.2025**	**1.5377**
JPEG #7	5.3483	5.4028	1.4807

Table 2: Performances of monoresolution lossless coding methods corresponding to the 256×256 "Boat" image (initial entropy $H_0 = 7.5747$).

Technique	H fixed	H adaptive
$(2,4)$	4.3779	4.3789
$(2,2)$	4.3621	4.3666
$(6,2)$	4.3295	4.3296
$(2+2,2)$	4.3253	4.3290
$(4,2)$	4.3191	4.3190
$(4,4)$	4.3160	4.3166
S	4.7912	4.7912
S+P	4.3499	4.3496
NL	4.3220	4.3244
NL$_*$	**4.3012**	**4.3038**

Table 3: Image "Lena", entropies of the 3-levels pyramids. For NL and NL*, when the predictors are fixed, they are obtained by the Neldear-Mead algorithm. For the LMS algorithm, $\mu = 5.10^{-5}, \lambda = 10^{-3}$. For NL*, the lowest resolution approximation sub-image is coded by a DPCM with a 3-th order optimal predictor.

Technique	H fixed	H adaptive
$(2,4)$	5.0069	5.0035
$(2,2)$	4.9815	4.9839
$(6,2)$	4.9252	4.9253
$(2+2,2)$	4.9186	4.9210
$(4,2)$	5.0875	4.9143
$(4,4)$	4.9287	4.9166
S	5.4606	5.4606
S+P	4.9863	4.9870
NL	4.9005	4.9009
NL$_*$	**4.8910**	**4.8918**

Table 4: Image "Boat", entropies of the 3-levels pyramids. For NL and NL*, when the predictors are fixed, they are obtained by the Neldear-Mead algorithm. For the LMS algorithm, $\mu = 5.10^{-5}, \lambda = 10^{-3}$. For NL*, the lowest resolution approximation sub-image is coded by a DPCM with a 3-th order optimal predictor.

Technique	r (bpp)	T_c
$(2,4)$	5.6470	1.4167
$(2,2)$	5.5471	1.4422
$(6,2)$	5.4767	1.4608
$(2+2,2)$	5.5948	1.4299
$(4,2)$	5.4802	1.4598
$(4,4)$	5.4939	1.4562
S	5.8407	1.3697
S+P	5.1433	1.5554
NL	5.4644	1.4645
NL*	**5.4354**	**1.4718**

Table 5: Image "Boat", bit rates and compression ratios of the 3-levels pyramids. All the predictors are fixed. For NL and NL*, the predictors are obtained by the Neldear-Mead algorithm. For NL*, the lowest resolution approximation sub-image is coded by a DPCM with a 3-th order optimal predictor.

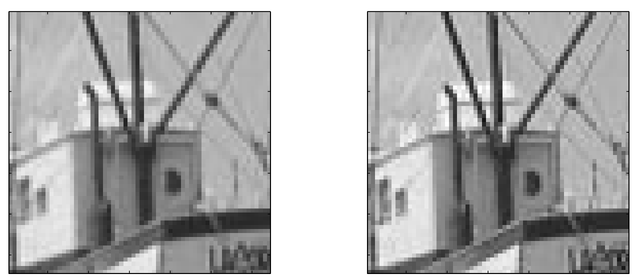

Figure 2: Image "Boat" , (left) S+P transform, (right) decomposition NL (optimized predictor), zoom of the approximation sub-image at level $j = 2$.